

# Hydrogen bond directed crystal engineering of nickel complexes: the effect of ligand methyl substituents on supramolecular structure

Matthew T. Allen, Andrew D. Burrows\* and Mary F. Mahon

Department of Chemistry, University of Bath, Claverton Down, Bath, UK BA2 7AY.  
 E-mail: a.d.burrows@bath.ac.uk

Received 30th September 1998, Accepted 16th November 1998

The interactions between two hydrogen bond donors and two hydrogen bond acceptors (DD:AA) have been used to form extended linear polymers based on bis(thiosemicarbazide)nickel(II) cations and terephthalate anions. In order to investigate the influence of the other hydrogen bond donors and acceptors present on these structures, the bis-(thiosemicarbazide)nickel(II) complexes  $trans\text{-}[\text{NiL}_2]^{2+}$ , where L is the methyl substituted thiosemicarbazides  $\text{L}^2$   $[\text{NHMeC}(\text{S})\text{NHNH}_2]$ ,  $\text{L}^3$   $[\text{NHMeC}(\text{S})\text{NHNMe}_2]$  and  $\text{L}^4$   $[\text{NH}_2\text{C}(\text{S})\text{NHNMe}_2]$ , have been prepared as terephthalate (tere) salts and their crystal structures investigated. The supramolecular structures of  $trans\text{-}[\text{Ni}(\text{L}^2)_2][\text{tere}]\cdot 4\text{H}_2\text{O}$  **2** and  $trans\text{-}[\text{Ni}(\text{L}^3)_2(\text{OH}_2)_2][\text{tere}]$  **3** show the expected  $\text{R}_2^2(8)$  motif linking the cations and anions into chains which are, in turn, cross-linked into sheets *via* amino  $\text{N-H}\cdots\text{O}$  hydrogen bonds in **2** and aqua  $\text{O-H}\cdots\text{O}$  hydrogen bonds in **3**. The supramolecular structure of  $trans\text{-}[\text{Ni}(\text{L}^4)_2(\text{OH}_2)_2][\text{tere}]\cdot 2\text{H}_2\text{O}$  **4**, in contrast, shows the absence of the expected cation  $\cdots$  anion  $\cdots$  cation chains. In this case, the cations and anions are linked by only one hydrogen bond, though interactions with the water molecules lead to an efficient hydrogen bonded structure with all potential hydrogen bond donors and acceptors involved in hydrogen bonding interactions. These structures demonstrate that the presence or absence of NH groups that are not involved in cation  $\cdots$  anion  $\cdots$  cation chain formation has a marked effect on both the nickel co-ordination geometry and the presence or absence of the anticipated linear hydrogen bonded chains.

## Introduction

In recent years there has been an enormous increase of interest in using supramolecular interactions as the basis for the attempted design of solid state structures, a process commonly referred to as crystal engineering.<sup>1</sup> The successes of crystal engineering have largely come about through the use of 'supramolecular synthons'.<sup>2</sup> By analogy with the synthons of organic synthesis, these 'supramolecular synthons' are small units, likely to interact with each other, or with other synthons, in a predictable or robust manner. These interactions can involve a number of different types of force, though the most commonly used of these is the hydrogen bond.<sup>3</sup>

The use of hydrogen bonds in crystal engineering has several advantages over the use of other intermolecular forces: hydrogen bonds are relatively strong and directional and they can act in concert with each other. By using complementary combinations of hydrogen bond donors and acceptors, Lehn<sup>4</sup> and Whitesides<sup>5</sup> have demonstrated that derivatives of melamine and cyanuric or barbituric acid co-crystallise as either extended tapes or discrete rosettes, depending on the steric requirements of the other substituents. Other combinations of donors and acceptors have also been employed in the design of organic solids<sup>3,6</sup> and a series of empirical rules<sup>7</sup> (Etter's rules) have been established for prediction of structures from the nature of the synthons. Complementary hydrogen bond interactions have been used as the basis of self-assembled tubular nanostructures,<sup>8</sup> imprinted polymers<sup>9</sup> and fluorescence probes.<sup>10</sup> In addition, the directionality of hydrogen bonds can be used in the generation of structures containing voids, since in a compound containing a symmetrical disposition of hydrogen bonding groups either close packing or hydrogen bonding potential has to be compromised.<sup>11</sup> Materials with such voids are of interest for both separation and catalytic applications.

Although most work in the past has focussed on the design of organic solids, the concepts have recently been extended into the inorganic domain.<sup>12</sup> Transition metal ions can be incorporated into hydrogen bonding networks by employing bifunctional ligands that contain, in addition to metal binding sites, hydrogen bonding functionalities that are retained on complexation.<sup>13</sup> As well as the potential harnessing of transition metal ion properties, the metal ion is able to act as a template, with the metal geometry dictating the relative orientation of ligands.

The strength of the interaction provided by sets of hydrogen bond donors and acceptors depends in part on the relative orientation of the hydrogen bonding groups. The interaction between a hydrogen bond donor–hydrogen bond donor (DD) set and a hydrogen bond acceptor–hydrogen bond acceptor (AA) set has been shown to be particularly robust since it contains only attractive secondary interactions,<sup>14</sup> and this combination has been used as the basis for dicarboxylate receptors in competitive solvents.<sup>15</sup> We have previously established<sup>16,17</sup> that the use of cations containing two DD sets from thiosemicarbazide ligands [thiosemicarbazide =  $\text{NH}_2\text{C}(\text{S})\text{NHNH}_2$ ,  $\text{L}^1$ ] together with dicarboxylate anions containing two AA sets leads to the formation of hydrogen bonded chains in the solid state even when the products are crystallised from a competitive solvent such as water. Identical chain formation occurs in  $trans\text{-}[\text{Ni}(\text{L}^1)_2][\text{tere}]$  **1** [tere = terephthalate,  $\text{C}_6\text{H}_4(\text{CO}_2^-)_2$ -1,4],<sup>16</sup>  $trans\text{-}[\text{Ni}(\text{L}^1)_2(\text{OH}_2)_2][\text{fum}]$  (fum = fumarate,  $trans\text{-}^-\text{O}_2\text{CCH}=\text{CHCO}_2^-$ )<sup>16</sup> and  $trans\text{-}[\text{Zn}(\text{L}^1)_2(\text{OH}_2)_2][\text{tere}]\cdot 2\text{H}_2\text{O}$ <sup>17</sup> through the DD:AA interaction (Fig. 1), which can be denoted as the *principal hydrogen bonds*. In all cases the chains interact together to give sheets, and the sheets interact to give three-dimensional structures through further hydrogen bonding involving the other N–H groups, carboxylate lone pairs and both free and co-ordinated water molecules. The cation and

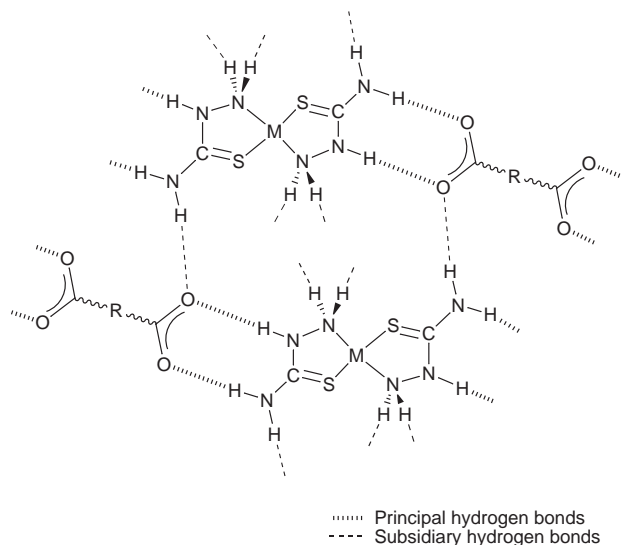
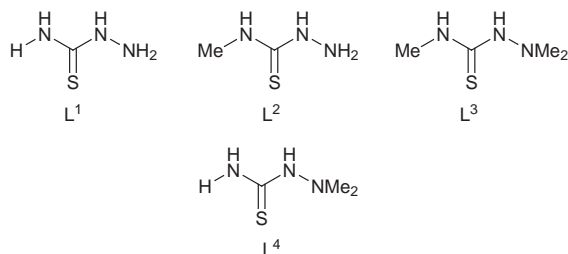


**Fig. 1** Principal and subsidiary hydrogen bond interactions between bis(thiosemicarbazide) complexes and dicarboxylates.

anion in all of these structures are essentially planar, and this coupled with the fact that sheet formation involves the coplanar thioamido proton leads to the sheets being nominally flat.

In this paper we explore the effects of the *subsidiary hydrogen bonds*, those not involved in chain formation, on the solid state structure. Towards this end, we have prepared and investigated nickel(II) complexes of the thiosemicarbazides  $RNHC(S)-NHNR'_2$  [ $L^2$   $R = Me$ ,  $R' = H$ ;  $L^3$   $R = Me$ ,  $R' = Me$ ;  $L^4$   $R = H$ ,  $R' = Me$ ] in which one or more NH hydrogen atoms involved in subsidiary hydrogen bond formation in **1** have been replaced by methyl groups. This does not affect the potential to form the cation...anion...cation chains, but does influence the way in which these chains can interact with each other. To aid structural comparisons, the cations were all crystallised with terephthalate anions from aqueous solution.



## Results and discussion

Single crystals of the terephthalate salts of  $trans-[Ni(L)_2]^{2+}$  ( $L = L^2, L^3, L^4$ ) were prepared by mixing aqueous solutions of sodium terephthalate and the appropriate bis(thiosemicarbazide)nickel(II) nitrate. In each case the single crystals were the only nickel-containing compounds formed, and the formula obtained by the crystal structure analysis was confirmed by microanalysis. These analyses confirmed the formulae of the compounds as  $trans-[Ni(L^2)_2][tere]\cdot 4H_2O$  **2**,  $trans-[Ni(L^3)_2](OH_2)_2[tere]$  **3** and  $trans-[Ni(L^4)_2](OH_2)_2[tere]\cdot 2H_2O$  **4**.

In the following discussions the cation plane is defined by atoms Ni, N(1) and S(1), the anion plane by the terephthalate aromatic ring and the sheet plane by the nickel atoms in the hydrogen bonded molecular sheet.

### Structure of $trans-[Ni(L^2)_2][tere]\cdot 4H_2O$ **2**

The asymmetric unit of compound **2**, as illustrated in the ORTEX<sup>18</sup> plot (Fig. 2) by the atoms with unprimed labels,

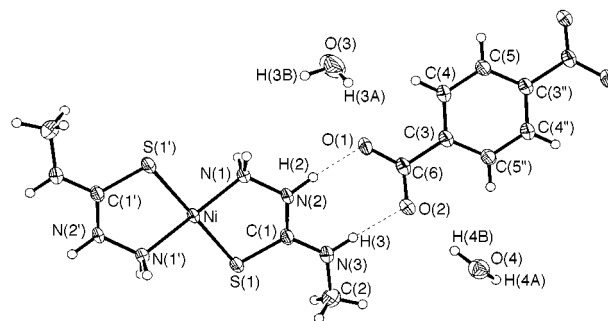


**Fig. 2** The asymmetric unit of compound **2**.

**Table 1** Selected bond lengths (Å) and angles (°) for **2**

Ni–N(1)	1.911(2)	N(1)–N(2)	1.429(3)
Ni–S(1)	2.1773(7)	N(2)–C(1)	1.321(3)
S(1)–C(1)	1.718(2)	N(3)–C(1)	1.316(3)
O(1)–C(6)	1.271(3)	N(3)–C(2)	1.443(4)
O(2)–C(6)	1.245(3)	C(3)–C(6)	1.511(3)
N(1)–Ni–S(1)	88.20(7)	N(3)–C(1)–S(1)	122.3(2)
N(1)–Ni–S(1')	91.80(7)	N(2)–C(1)–S(1)	119.7(2)
N(2)–N(1)–Ni	114.5(2)	O(2)–C(6)–O(1)	124.9(2)
C(1)–N(2)–N(1)	117.8(2)	O(2)–C(6)–C(3)	118.9(2)
C(1)–N(3)–C(2)	123.5(2)	O(1)–C(6)–C(3)	116.2(2)
N(3)–C(1)–N(2)	118.0(2)		

Equivalent atoms labelled ' are generated *via* the symmetry transformation  $-x, -y, -z$ .

consists of one half of a cation, one half of an anion and two included water molecules. The nickel atom is positioned at 0, 0, 0 with a site occupancy of 0.5, and an inversion centre at this position serves to generate the remaining portion of the cationic complex. Similarly, the anion straddles another inversion centre, at  $-0.5, 0, -1$ , which yields the symmetry related portion.

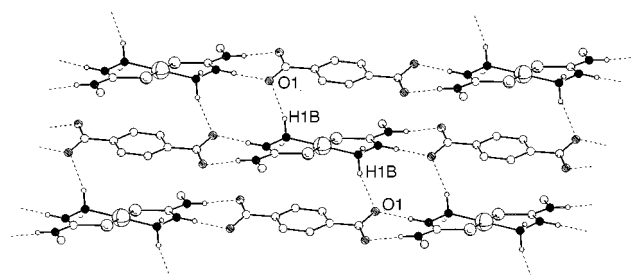
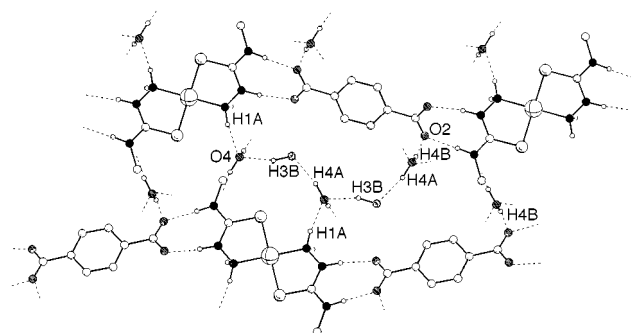
The nickel co-ordination geometry in **2** is distorted square planar, and selected bond lengths and angles are given in Table 1. The Ni–N and Ni–S distances are all slightly longer than those observed for the  $[Ni(L^1)_2]^{2+}$  cation in the crystal structure of  $[Ni(L^1)_2][tere]$  **1**.<sup>16</sup> In contrast to **1**, in which the pseudo-axial positions of the square planar cation are occupied by the  $\pi$ -systems of terephthalate anions, the corresponding positions in **2** are unoccupied. In the anion the carboxylate groups are rotated out of the plane of the aromatic ring, the mean torsional twist about C(6)–C(3) being 14.5°.

Details of the hydrogen bonding within the supramolecular structure are given in Table 2. The cations are linked to the terephthalate anions through the anticipated two principal hydrogen bonds between N(2)–H(2) and O(1), and N(3)–H(3) and O(2) respectively. These interactions lead to the formation of 8-membered hydrogen bonded rings [graph set  $R_2^2(8)$ ] and consequently, to infinite cation...anion...cation chains through the gross structure (Fig. 3). An additional longer (and less directional) hydrogen bond between one of the amino hydrogen atoms, H(1B), and a terephthalate oxygen atom, O(1), serves to inter-link these linear polymers into sheets with formation of 10- and 30-membered hydrogen-bonded rings (Fig. 3). In contrast to the structure of  $[Ni(L^1)_2][tere]$  **1**,<sup>16</sup> neither the cations nor anions in **2** lie flat within the sheets. This is a direct consequence of the involvement of one of the amino protons on N(1) in sheet formation, as these protons are directed above and below the cation plane, and is reflected in the angles between the planes defined by the cations and anions and that defined by the sheets, which are 71.3(1) and 58.8(1)° respectively.

A second type of intermolecular interaction results from the presence of the water molecules, and these link the sheets

**Table 2** Hydrogen bond geometries in the crystal structure of **2**

X–H···Y	X···Y/Å	H···Y/Å	X–H···Y/°	Symmetry operation generating Y
Within sheets				
N(2)–H(2)···O(1)	2.767(3)	1.82(2)	172(3)	
N(3)–H(3)···O(2)	2.804(3)	1.87(2)	176(3)	
N(1)–H(1B)···O(1)	2.956(3)	2.05(2)	161(2)	$-x, -y, -1 - z$
Between sheets				
N(1)–H(1A)···O(4)	2.880(3)	1.96(2)	166(2)	$-1 - x, -y, -1 - z$
O(4)–H(4A)···O(3)	2.777(3)	1.87(2)	166(3)	$-1 - x, 0.5 + y, -1.5 - z$
O(4)–H(4B)···O(2)	2.825(3)	1.92(2)	164(3)	
O(3)–H(3B)···O(4)	2.806(3)	1.92(3)	153(4)	$-1 - x, -y, -1 - z$

**Fig. 3** Part of the hydrogen bonded sheets present in the structure of compound **2**.**Fig. 4** Interactions between the sheets in the structure of compound **2**.

together (Fig. 4). The amino hydrogen atom H(1A) hydrogen bonds to the oxygen atom O(4) of the water molecule that contains the hydrogen atoms H(4A) and H(4B). These protons, in turn, form contacts to the water oxygen atom O(3) and terephthalate oxygen atom O(2) respectively. Finally, H(3B) in one of the water molecules hydrogen bonds to the oxygen atom of the other water molecule O(4), the second hydrogen bond that this atom accepts.<sup>19</sup> The remaining proton in this water molecule [H(3A)] is not involved in any intermolecular interactions.

### Structure of *trans*-[Ni(L<sup>3</sup>)<sub>2</sub>(OH<sub>2</sub>)<sub>2</sub>][tere] **3**

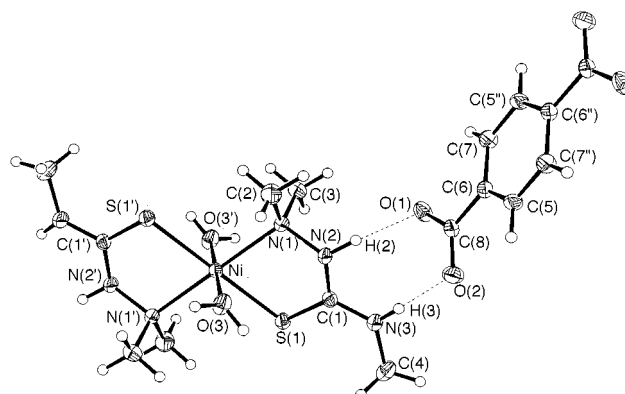
The asymmetric unit of compound **3**, as illustrated in the ORTEX plot (Fig. 5) by the labelled unprimed atoms, consists of one half of a cation and one half of an anion. The remainder of the cation is generated by transformation through the inversion centre at 0, 0, 0 (the nickel atom location, site occupancy 0.5), while the anion is completed by transformation through the inversion centre at  $-1, 0.5, -0.5$ .

The nickel co-ordination geometry of compound **3** is distorted octahedral, with water molecules occupying the axial sites. Selected bond lengths and angles are given in Table 3. The Ni–N and Ni–S distances are, as expected, longer than those in **2** due to the increase in co-ordination number. The parameters in **3** are much closer to those in [Ni(L<sup>1</sup>)<sub>2</sub>(OH<sub>2</sub>)<sub>2</sub>][fum],<sup>16</sup> though the Ni–N distance is considerably longer [2.190(2) Å *cf.*

**Table 3** Selected bond lengths (Å) and angles (°) for **3**

Ni–O(3)	2.090(2)	N(2)–C(1)	1.350(3)
Ni–N(1)	2.190(2)	N(3)–C(1)	1.323(3)
Ni–S(1)	2.3801(8)	N(3)–C(3)	1.448(3)
S(1)–C(1)	1.702(2)	O(1)–C(8)	1.261(2)
N(1)–N(2)	1.432(2)	O(2)–C(8)	1.250(2)
N(1)–C(2)	1.479(3)	C(6)–C(8)	1.509(3)
N(1)–C(3)	1.484(3)		
O(3)–Ni–N(1)	85.85(6)	C(1)–N(2)–N(1)	120.2(2)
O(3)–Ni–S(1)	89.36(5)	C(1)–N(3)–C(3)	124.2(2)
O(3)–Ni–S(1')	90.64(5)	N(3)–C(1)–N(2)	114.5(2)
O(3)–Ni–N(1')	94.15(6)	N(3)–C(1)–S(1)	122.9(2)
N(1)–Ni–S(1)	81.97(5)	N(2)–C(1)–S(1)	122.58(14)
N(1)–Ni–S(1')	98.03(5)	O(2)–C(8)–O(1)	123.9(2)
C(1)–S(1)–Ni	95.36(7)	O(2)–C(8)–C(6)	119.5(2)
N(2)–N(1)–Ni	107.88(11)	O(1)–C(8)–C(6)	116.6(2)

Equivalent atoms labelled ' are generated *via* the symmetry transformation  $-x, -y, -z$ .

**Fig. 5** The asymmetric unit of compound **3**.

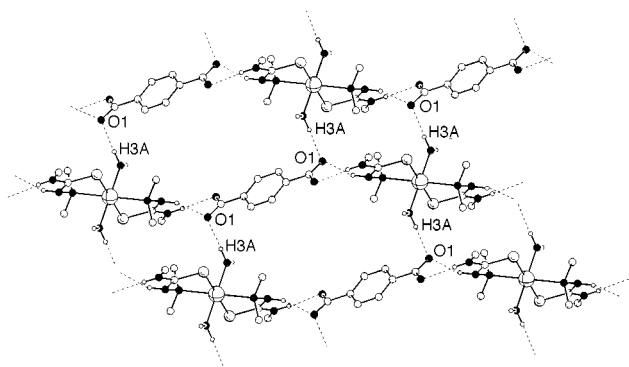
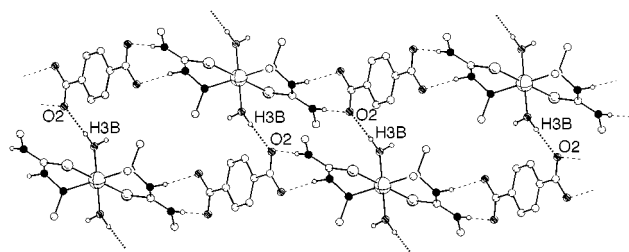
2.093(2) Å], consistent with the weaker co-ordination of the tertiary amine nitrogen atom. As in **2** the carboxylate groups of the terephthalate anion are rotated out of the plane of the aromatic ring, the mean torsional twist around C(8)–C(6) being 9.5°.

The hydrogen bonds present within the structure of **3** are summarised in Table 4. Once again the supramolecular structure is dominated by the two principal hydrogen bonds between each co-ordinated L<sup>3</sup> ligand and carboxylate group [graph set R<sub>2</sub><sup>2</sup>(8)] which serve to link the ions into infinite cation···anion···cation chains. The interaction between N(3)–H(3) and O(2) is considerably longer than that between N(2)–H(2) and O(1), though the longer bond is more directional. There is considerable twisting of the chains, and this is reflected in the angle between the cation and anion planes, which is surprisingly large [75.9(1)°].

Ligand L<sup>3</sup> has only two N–H functionalities, both of which are tied up in chain formation. In the absence of further N–H

**Table 4** Hydrogen bond geometries in the crystal structure of **3**

X–H···Y	X···Y/Å	H···Y/Å	X–H···Y/°	Symmetry operation generating Y
Within sheets				
N(2)–H(2)···O(1)	2.767(2)	1.89(2)	162(2)	1 + x, y, z
N(3)–H(3)···O(2)	2.925(2)	2.04(2)	178(2)	
O(3)–H(3A)···O(1)	2.799(2)	1.93(2)	174(3)	
Between sheets				
O(3)–H(3B)···O(2)	2.749(2)	1.89(2)	170(3)	–1 – x, – y, –1 – z

**Fig. 6** Part of the hydrogen bonded sheets present in the structure of compound **3**.**Fig. 7** Interactions between the sheets in the structure of compound **3**.

groups, the linking of chains into sheets has to occur *via* another means. In this compound it occurs *via* a hydrogen bond from a proton on the axial co-ordinated water molecule [H(3A)] to the carboxylate oxygen atom O(1), which results in formation of both 14- and 30-membered hydrogen bonded rings (Fig. 6). The use of an aqua proton to link the chains into sheets means that, as in **2**, the cations and anions do not lie flat within the sheets, and this is evidenced by the angles between the cation and anion planes and that of the sheets which are 62.3(1) and 57.9(1)° respectively.

An additional hydrogen bond between the carboxylate oxygen atom O(2) and the second aqua proton H(3B) serves to link the sheets into a three-dimensional network (Fig. 7).

#### Structure of *trans*-[Ni(L<sup>4</sup>)<sub>2</sub>(OH)<sub>2</sub>][tere]·2H<sub>2</sub>O **4**

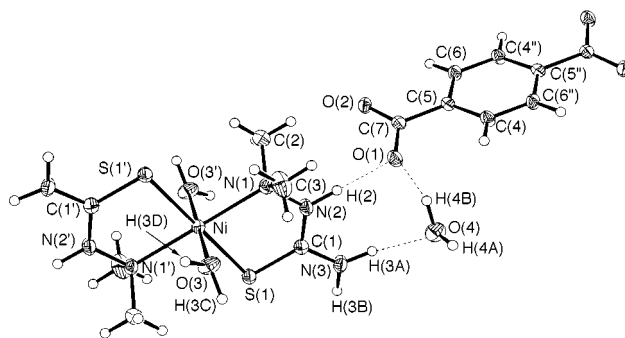
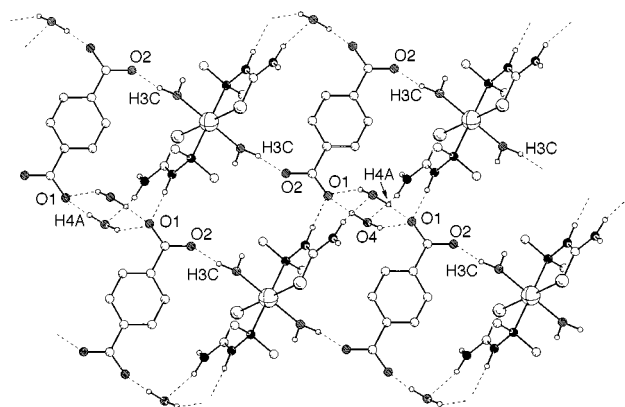
The asymmetric unit of compound **4**, as illustrated in the ORTEP plot (Fig. 8) by the labelled unprimed atoms, consists of one half of a cation, one half of an anion and one included water molecule. The nickel atom is positioned at 0, 0, 0 with a site occupancy of 0.5, and an inversion centre at this position serves to generate the remaining portion of the cationic complex. The anion straddles another inversion centre at 0.5, 0.5, –1 which yields the symmetry related portion.

The nickel co-ordination geometry in **4** is distorted octahedral with water molecules occupying the axial sites as in **3**. Selected bond lengths and angles are given in Table 5. The Ni–N distance, at 2.219(2) Å, is somewhat longer than that

**Table 5** Selected bond lengths (Å) and angles (°) for **4**

Ni–O(3)	2.113(2)	N(1)–C(3)	1.482(4)
Ni–N(1)	2.219(2)	N(2)–C(1)	1.325(3)
Ni–S(1)	2.3252(7)	N(3)–C(1)	1.332(3)
S(1)–C(1)	1.702(2)	O(1)–C(7)	1.277(3)
N(1)–N(2)	1.431(3)	O(2)–C(7)	1.248(3)
N(1)–C(2)	1.480(4)	C(7)–C(5)	1.508(3)
O(3)–Ni–N(1')	90.57(8)	N(2)–N(1)–Ni	110.5(2)
O(3)–Ni–N(1)	89.43(8)	C(1)–N(2)–N(1)	122.3(2)
O(3)–Ni–S(1')	89.49(6)	N(2)–C(1)–S(1)	124.1(2)
N(1)–Ni–S(1')	95.60(6)	O(2)–C(7)–O(1)	123.0(2)
O(3)–Ni–S(1)	90.51(6)	O(2)–C(7)–C(5)	119.4(2)
N(1)–Ni–S(1)	84.40(6)	O(1)–C(7)–C(5)	117.5(2)
C(1)–S(1)–Ni	98.35(9)		

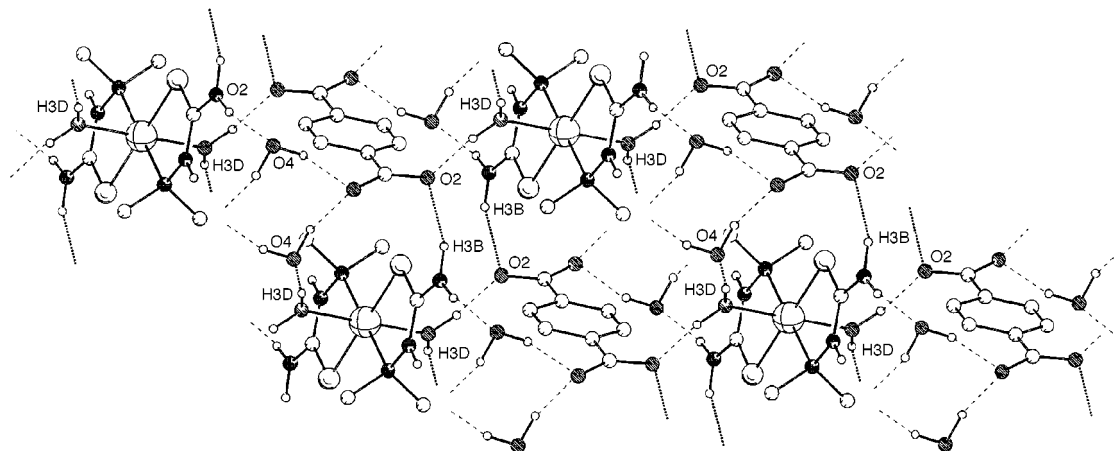
Equivalent atoms labelled ' are generated *via* the symmetry transformation –x, –y, –z.

**Fig. 8** The asymmetric unit of compound **4**.**Fig. 9** Part of the hydrogen bonded sheets present in the structure of compound **4**.

in **3** whereas the Ni–S distance, at 2.3252(7) Å, is somewhat shorter. These changes in co-ordination geometry are also reflected in an increase in the N–Ni–S bite angle to 84.40(6)°, *cf.* 81.97(5)° for **3**. The carboxylate groups of the terephthalate anion are again rotated out of the plane of the aromatic ring, the mean torsional twist around C(7)–C(5) being 10.3°.

**Table 6** Hydrogen bond geometries in the crystal structure of **4**

X–H···Y	X···Y/Å	H···Y/Å	X–H···Y/°	Symmetry operation generating Y
Within sheets				
N(2)–H(2)···O(1)	2.837(3)	1.860(4)	175(3)	
N(3)–H(3A)···O(4)	3.042(3)	2.083(9)	166(3)	
O(4)–H(4B)···O(1)	2.775(3)	1.88(2)	151(4)	
O(3)–H(3C)···O(2)	2.719(3)	1.748(7)	170(3)	$x, y, 1 + z$
O(4)–H(4A)···O(1)	2.864(3)	1.91(1)	165(3)	$1 - x, 1 - y, -1 - z$
Between sheets				
N(3)–H(3B)···O(2)	2.963(3)	2.03(1)	159(3)	$1 - x, -y, -1 - z$
O(3)–H(3D)···O(4)	2.812(3)	1.839(7)	171(4)	$-1 + x, y, 1 + z$

**Fig. 10** Interactions between the sheets in the structure of compound **4**.

The major surprise provided by the crystal structure of **4** involves the supramolecular structure, as the expected DD:AA hydrogen bond links between the thiosemicarbazide and carboxylate groups are not present. This leads to an absence of the infinite cation···anion···cation chains present in all the other complexes of this type, and the structure of **4** is best described in terms of sheets running in the (1–10) planes of the crystal (Fig. 9). The hydrogen bonds present within the structure of **4** are summarised in Table 6. There is a single hydrogen bond between a thiosemicarbazide NH group N(2)–H(2) and terephthalate oxygen atom O(1) in the expected orientation but instead of being virtually co-planar, the planes of the two ions are almost perpendicular [79.1(2)°]. The NH group parallel to the N(2)–H(2) vector [*i.e.* N(3)–H(3A)] is involved in hydrogen bonding, but to an oxygen atom from an included water molecule [O(4)] rather than the terephthalate. The second carboxylate oxygen atom O(2) hydrogen bonds to the hydrogen atom H(3C) of a bound water molecule in another asymmetric unit. Additional hydrogen bonds between the carboxylate oxygen atom O(1) and both hydrogen atoms H(4A) and H(4B) from the included water molecule serve to link terephthalate anions through  $R_4^2(8)$  rings and complete the hydrogen bonding within the sheets. Each O(1) carboxylate oxygen atom acts as a hydrogen bond acceptor to three protons. The absence of the expected principal hydrogen bonds leads to the major first order motifs being those described by the graph sets  $R_3^2(8)$  and  $R_4^2(8)$ , as opposed to  $R_2^2(8)$  as in the structures of **1**, **2** and **3**. Of the hydrogen bonded rings present in the structure of **4**,  $R_4^2(8)$  is very common in hydrogen bonded structures<sup>3</sup> whereas the  $R_3^2(8)$  motif is somewhat more unusual. Larger 17- and 18-membered hydrogen-bonded rings are also present.

Two further hydrogen bond interactions link the sheets into the final three-dimensional network (Fig. 10). The remaining amino proton H(3B) links to a terephthalate anion oxygen atom O(2), and the second proton on the co-ordinated water

H(3D) links to the included water oxygen atom O(4). Overall all hydrogen bond donors and acceptors are satisfied.

#### Comparison of the structures of 1–4

This series of compounds, prepared under identical conditions, contains nickel(II) in either a distorted square planar (**1** and **2**) or octahedral (**3** and **4**) geometry, depending on the absence or presence of axially co-ordinated water molecules. Water is a versatile component in these systems with the potential to act as both hydrogen bond donor and acceptor as well as ligand. Hence, the presence of water molecules, either co-ordinated or included in the lattice, is likely to be dictated by the energy requirements of the crystal structure as a whole. A ligand such as  $L^3$  has a paucity of hydrogen bond donors, all of which are involved in chain formation. Hence any compound of the type  $[\text{Ni}(L^3)_2][\text{dica}]$  (dica = dicarboxylate) will contain four ‘unsatisfied’ hydrogen bond acceptors per dicarboxylate. The introduction of co-ordinated water increases the number of hydrogen bond donors, hence compounds of the type  $[\text{Ni}(L^3)_2(\text{OH}_2)_2][\text{dica}]$  are likely to form more efficient hydrogen bonded structures than  $[\text{Ni}(L^3)_2][\text{dica}]$ . This is supported not only by the crystal structure of **3**, but also by the crystal structure of  $[\text{Ni}(L^3)_2(\text{OH}_2)_2][\text{A}]$  [A = isophthalate,  $\text{C}_6\text{H}_4(\text{CO}_2^-)_{2-1,3}$ ].<sup>20</sup> The presence or absence of hydrogen bonding sites within the ligands can therefore have an effect on the metal co-ordination geometry, at least in cases where the energy difference between alternative geometries is relatively small.

Compounds **1**, **2** and **3** all possess structures in which the DD:AA ‘principal’ hydrogen bond interactions serve to link the cations and anions into infinite chains. These hydrogen bonds, giving rise to  $R_2^2(8)$  rings, are fairly flexible as witnessed by the amount of twisting observed in the structures. This twisting of the DD:AA motif can be quantified by the angle made by superimposing the O···O vector of the carboxylate onto the N···N vector of the thiosemicarbazide [the

**Table 7** Crystallographic data for compounds **2**, **3** and **4**

Complex	<b>2</b>	<b>3</b>	<b>4</b>
Empirical formula	C <sub>12</sub> H <sub>26</sub> N <sub>6</sub> O <sub>8</sub> S <sub>2</sub> Ni	C <sub>16</sub> H <sub>30</sub> N <sub>6</sub> O <sub>6</sub> S <sub>2</sub> Ni	C <sub>14</sub> H <sub>30</sub> N <sub>6</sub> O <sub>8</sub> S <sub>2</sub> Ni
<i>M</i>	473.22	525.29	533.28
Crystal system	Monoclinic	Triclinic	Triclinic
Space group	<i>P</i> 2 <sub>1</sub> / <i>c</i> (no. 14)	<i>P</i> $\bar{1}$ (no. 2)	<i>P</i> $\bar{1}$ (no. 2)
<i>a</i> /Å	7.668(1)	8.107(1)	8.215(1)
<i>b</i> /Å	15.926(2)	8.108(2)	8.344(1)
<i>c</i> /Å	8.951(1)	9.675(2)	8.888(1)
$\alpha$ /°		93.52(2)	88.30(1)
$\beta$ /°	100.25(1)	113.86(2)	66.78(1)
$\gamma$ /°		90.10(2)	83.19(1)
<i>U</i> /Å <sup>3</sup>	1075.7(2)	580.3(2)	555.8(1)
<i>Z</i>	2	1	1
<i>D</i> <sub>c</sub> /g cm <sup>-3</sup>	1.560	1.503	1.593
$\mu$ (Mo-K $\alpha$ )/mm <sup>-1</sup>	1.146	1.060	1.114
<i>F</i> (000)	528	276	280
Crystal size/mm	0.25 × 0.25 × 0.2	0.5 × 0.25 × 0.25	0.2 × 0.2 × 0.3
Index ranges	0–8, –18 to 0, –10 to 10	–9 to 9, 0–9, –11 to 11	0–9, –9 to 9, –9 to 10
No. data collected	1824	1956	1882
<i>R</i> (int)	0.0102	0.0074	0.0177
Data, restraints, parameters	1688, 8, 159	1809, 4, 162	1741, 7, 173
Goodness-of-fit	1.132	1.055	0.968
<i>R</i> 1, <i>wR</i> 2 [ <i>I</i> > 2 $\sigma$ ( <i>I</i> )]	0.0282, 0.0696	0.0218, 0.0607	0.0272, 0.0648
<i>R</i> indices (all data)	0.0428, 0.0777	0.0263, 0.0639	0.0414, 0.0722
Largest difference peak, hole/e Å <sup>-3</sup>	0.404, –0.298	0.290, –0.265	0.257, –0.203
Weighting scheme, <i>w</i> <sup>-1</sup> , where <i>P</i> = ( <i>F</i> <sub>o</sub> <sup>2</sup> + 2 <i>F</i> <sub>c</sub> <sup>2</sup> )/3	$\sigma^2(F_o^2) + (0.0425P)^2 + 0.5615P$	$\sigma^2(F_o^2) + (0.0393P)^2 + 0.2807P$	$\sigma^2(F_o^2) + (0.0406P)^2 + 0.3965P$
Extinction coefficient	0.0142(15)	0.0369(32)	0.0019(24)
Details in common: $\lambda$ (Mo-K $\alpha$ ) 0.71069 Å, <i>T</i> = 293(2) K, $\theta$ range 2–24°			

N(3)···N(2)···O(1)···O(2) torsion angle in **2** and **3**], which gives values of 6.1° for **1**, 22.4(1)° for **2** and 48.0(1)° for **3**. The deviations from 0° occur presumably due to the other demands made upon the ions, as the overall lowest energy structure is a compromise taking into account all interactions. However, the flexibility of supramolecular synthons such as the DD:AA interaction is a factor in the frequency of their occurrence. This twisting is also a factor in the large angle between the cation and anion planes in **3** [75.9(1)°, *cf.* 16.2° for **1** and 15.4(2)° for **2**].

In compounds **1**, **2** and **3** the hydrogen bonded chains are linked to form sheets. In **1** this occurs through the thioamido proton that is not involved in chain formation, and since this NH bond is orientated in essentially the same plane as the metal co-ordination sphere, the plane described by the sheets is similar to those described by the ions. The cation plane–sheet and anion plane–sheet angles are 16.4 and 9.5° respectively. In **2** the thioamido proton has been substituted by a methyl group, and consequently it is an amino proton that serves to hydrogen bond the chains into sheets. Since this NH vector is not directed in the plane of the cation, the planes described by the ions are much less co-planar with those of the sheets: the cation plane–sheet and anion plane–sheet angles are 71.3(1) and 58.8(1)° respectively. In **3** there are no NH protons available for cross linking the chains, and hence sheet formation occurs *via* OH protons on axially co-ordinated aqua ligands. This leads once more to large differences between the planes described by the ions and that described by the sheets, with the cation plane–sheet and anion plane–sheet angles 62.3(1) and 57.9(1)° respectively.

Compound **4**, like **1**, contains a thioamido proton and appears to be set up to form strongly hydrogen bonded sheets, with the ions essentially co-planar with the plane of the sheets. However, as has been observed, this structure does not occur and indeed cation···anion···cation chain formation through the expected principal hydrogen bond interactions is not present. Despite not forming the predicted structure, it should be noted that all of the potential hydrogen bond donors and acceptors are involved in strong hydrogen bonds, suggesting the overall three-dimensional structure is very efficient. Although the expected planar two-dimensional structure for **4** would be

efficient, presumably these sheets would not be able to pack together as well, leading to a less favourable structure overall.

This series of relatively simple salts has demonstrated that both the metal co-ordination geometry and the presence or absence of robust supramolecular synthons can be affected by the presence or absence of other hydrogen bonding groups. Hence structural predictions based only upon principal hydrogen bond interactions may not always give rise to the observed structures.

## Experimental

Microanalyses were carried out by Mr Alan Carver (University of Bath Microanalytical Service). Infrared spectra were recorded on a Nicolet 510P spectrometer as KBr pellets. Sodium terephthalate and L<sup>2</sup> were purchased from Aldrich Chemical Co. and used as supplied, and the ligands L<sup>3</sup> and L<sup>4</sup> were prepared following literature procedures.<sup>21</sup> The complexes [Ni(L)<sub>2</sub>(ONO<sub>2</sub>)<sub>2</sub>] were prepared from the reaction of [Ni(NO<sub>3</sub>)<sub>2</sub>·6H<sub>2</sub>O] with the relevant thiosemicarbazide in ethanol<sup>22</sup> and used without further purification.

In the syntheses of **2**, **3** and **4**, yields of around 60% were obtained under the conditions mentioned, though yields of 90% could be obtained on leaving the solutions for longer periods of time.

### Synthesis of [Ni(L<sup>2</sup>)<sub>2</sub>][tere]·4H<sub>2</sub>O **2**

An aqueous solution of sodium terephthalate (53.5 mg, 0.25 mmol) was added to an aqueous solution of [Ni(L<sup>2</sup>)<sub>2</sub>(ONO<sub>2</sub>)<sub>2</sub>] (100 mg, 0.25 mmol). After standing for 24 h, red crystals of [Ni(L<sup>2</sup>)<sub>2</sub>][tere]·4H<sub>2</sub>O were separated by filtration. (Found: N, 16.5; C, 28.8; H, 5.09. C<sub>12</sub>H<sub>26</sub>N<sub>6</sub>NiO<sub>8</sub>S<sub>2</sub> requires N, 16.6; C, 28.5; H, 5.19%;  $\nu_{\max}/\text{cm}^{-1}$ (CO<sub>2</sub>) 1559s, 1356s;  $\nu_{\max}/\text{cm}^{-1}$ (NH) 3441m, 3256m;  $\delta_{\max}/\text{cm}^{-1}$ (NH) 1669m, 1624m.

### Synthesis of [Ni(L<sup>3</sup>)<sub>2</sub>(OH)<sub>2</sub>][tere] **3**

An aqueous solution of sodium terephthalate (47 mg, 0.22 mmol) was added to an aqueous solution of [Ni(L<sup>3</sup>)<sub>2</sub>(ONO<sub>2</sub>)<sub>2</sub>] (100 mg, 0.22 mmol). After standing for 24 h, green crystals of

[Ni(L<sup>3</sup>)<sub>2</sub>(OH<sub>2</sub>)<sub>2</sub>][tere] were separated by filtration (Found: N, 15.7; C, 36.4; H, 5.80. C<sub>16</sub>H<sub>30</sub>N<sub>6</sub>NiO<sub>6</sub>S<sub>2</sub> requires N, 16.0; C, 36.6; H, 5.76%);  $\nu_{\max}/\text{cm}^{-1}(\text{CO}_2)$  1561s, 1372s;  $\nu_{\max}/\text{cm}^{-1}(\text{NH})$  3240m;  $\delta_{\max}/\text{cm}^{-1}(\text{NH})$  1615m.

#### Synthesis of [Ni(L<sup>4</sup>)<sub>2</sub>(OH<sub>2</sub>)<sub>2</sub>][tere]·2H<sub>2</sub>O **4**

An aqueous solution of sodium terephthalate (50 mg, 0.24 mmol) was added to an aqueous solution of [Ni(L<sup>4</sup>)<sub>2</sub>(ONO<sub>2</sub>)<sub>2</sub>] (100 mg, 0.24 mmol). After standing for 24 h, green crystals of [Ni(L<sup>4</sup>)<sub>2</sub>(OH<sub>2</sub>)<sub>2</sub>][tere]·2H<sub>2</sub>O were separated by filtration. (Found: N, 15.5; C, 31.7; H, 5.65. C<sub>14</sub>H<sub>30</sub>N<sub>6</sub>NiO<sub>8</sub>S<sub>2</sub> requires N, 15.8; C, 31.5; H, 5.67%);  $\nu_{\max}/\text{cm}^{-1}(\text{CO}_2)$  1560s, 1360s;  $\nu_{\max}/\text{cm}^{-1}(\text{NH})$  3339m, 3190m;  $\delta_{\max}/\text{cm}^{-1}(\text{NH})$  1643m.

#### Crystallography

Table 7 provides a summary of the crystal data, data collection and refinement parameters for complexes **2**, **3** and **4**. In all cases, in the final least-squares cycles all atoms were allowed to vibrate anisotropically. The hydrogen atoms were included in calculated positions where relevant on carbon atoms, whereas the remaining hydrogen atoms were located and refined at a fixed distance of 0.98 Å from the relevant parent atoms. Calculations were carried out using SHELXS-86<sup>23</sup> (structure solutions) and SHELXL-93<sup>24</sup> (refinements). All full matrix least-squares refinements were based on *F*<sup>2</sup> data.

CCDC reference number 186/1254.

#### Acknowledgements

The University of Bath is thanked for financial support.

#### References

- 1 *Comprehensive Supramolecular Chemistry*, ed. J. L. Atwood, J. E. D. Davies, D. D. MacNicol and F. Vögtle, Pergamon, Oxford, 1996, vol. 6 is devoted to crystal engineering.
- 2 G. R. Desiraju, *Angew. Chem., Int. Ed. Engl.*, 1995, **34**, 2311; V. R. Thalladi, B. S. Goud, V. J. Hoy, F. H. Allen, J. A. K. Howard and G. R. Desiraju, *Chem. Commun.*, 1996, 401.
- 3 J. C. MacDonald and G. M. Whitesides, *Chem. Rev.*, 1994, **94**, 2383; C. B. Aakeröy and K. R. Seddon, *Chem. Soc. Rev.*, 1993, **22**, 397; M. Mascal, *Contemp. Org. Synth.*, 1994, **1**, 31.
- 4 J.-M. Lehn, M. Mascal, A. DeCian and J. Fischer, *J. Chem. Soc., Perkin Trans. 2*, 1992, 461.

- 5 G. M. Whitesides, E. E. Simanek, J. P. Mathias, C. T. Seto, D. N. Chin, M. Mammen and D. M. Gordan, *Acc. Chem. Res.*, 1995, **28**, 37; J. A. Zerkowski and G. M. Whitesides, *J. Am. Chem. Soc.*, 1994, **116**, 4298.
- 6 J. van Esch, S. de Feyter, R. M. Kellogg, F. de Schryver and B. L. Feringa, *Chem. Eur. J.*, 1997, **3**, 1238.
- 7 M. C. Etter, *Acc. Chem. Res.*, 1990, **23**, 120; M. C. Etter, *J. Phys. Chem.*, 1991, **95**, 4601; J. Bernstein, R. E. Davis, L. Shimoni and N.-L. Chang, *Angew. Chem., Int. Ed. Engl.*, 1995, **34**, 1555.
- 8 N. Kimizuka, T. Kawasaki, K. Hirata and T. Kunitake, *J. Am. Chem. Soc.*, 1995, **117**, 6360; N. Kimizuka, S. Fujikawa, H. Kuwahara, T. Kunitake, A. Marsh and J.-M. Lehn, *J. Chem. Soc., Chem. Commun.*, 1995, 2103.
- 9 K. Tanabe, T. Takeuchi, J. Matsui, K. Ikebukuro, K. Yano and I. Karube, *J. Chem. Soc., Chem. Commun.*, 1995, 2303.
- 10 K. Motesharei and D. C. Myles, *J. Am. Chem. Soc.*, 1994, **116**, 7413.
- 11 S. V. Kolotuchin, E. E. Fenlon, S. R. Wilson, C. J. Loweth and S. C. Zimmerman, *Angew. Chem., Int. Ed. Engl.*, 1995, **34**, 2654; O. M. Yaghi, H. Li and T. L. Groy, *J. Am. Chem. Soc.*, 1996, **118**, 9096; R. E. Melendez, C. V. K. Sharma, M. J. Zaworotko, C. Bauer and R. D. Rogers, *Angew. Chem., Int. Ed. Engl.*, 1996, **35**, 2213; M. Fujita and K. Ogura, *Coord. Chem. Rev.*, 1996, **148**, 249.
- 12 D. Braga, F. Grepioni and G. R. Desiraju, *Chem. Rev.*, 1998, **98**, 1375; S. Subramanian and M. J. Zaworotko, *Coord. Chem. Rev.*, 1994, **137**, 357.
- 13 A. D. Burrows, C.-W. Chan, M. M. Chowdhry, J. E. McGrady and D. M. P. Mingos, *Chem. Soc. Rev.*, 1995, **24**, 329;
- 14 J. Pranata, S. G. Wierschke and W. L. Jorgensen, *J. Am. Chem. Soc.*, 1991, **113**, 2810.
- 15 E. Fan, S. A. van Arman, S. Kincaid and A. D. Hamilton, *J. Am. Chem. Soc.*, 1993, **115**, 369; M. S. Goodman, V. Jubian and A. D. Hamilton, *Tetrahedron Lett.*, 1995, **36**, 2551.
- 16 A. D. Burrows, D. M. P. Mingos, A. J. P. White and D. J. Williams, *Chem. Commun.*, 1996, 97.
- 17 A. D. Burrows, S. Menzer, D. M. P. Mingos, A. J. P. White and D. J. Williams, *J. Chem. Soc., Dalton Trans.*, 1997, 4237.
- 18 P. McArdle, *J. Appl. Crystallogr.*, 1994, **27**, 438.
- 19 G. A. Jeffrey and H. Maluszynska, *Acta Crystallogr. Sect. B*, 1990, **46**, 546.
- 20 A. D. Burrows and M. F. Mahon, unpublished work.
- 21 K. A. Jensen, U. Anthoni, B. Kägi, C. Larsen and C. T. Pedersen, *Acta Chem. Scand.*, 1968, **22**, 1.
- 22 K. A. Jensen and E. Rancke-Madsen, *Z. Anorg. Allg. Chem.*, 1934, **219**, 243.
- 23 G. M. Sheldrick, *Acta Crystallogr. Sect. A*, 1990, **46**, 467.
- 24 G. M. Sheldrick, SHELXL-93, a computer program for crystal structure refinement, University of Göttingen, 1993.

Paper 8/07601D